Paper No. 961. (quote when citing this article)
Eleventh World Conference on Earthquake Engineering
ISBN: 0 08 042822 3

ABSOLUTE ACCELERATION MEASUREMENT BASED H$^\infty$ STRUCTURAL CONTROL SYSTEM DESIGN

N. YAMADA and A. NISHITANI

Department of Architecture, Waseda University,
3-4-1 Okubo Shinjuku-ku, Tokyo 169, Japan

ABSTRACT

This paper discusses the H$^\infty$ structural control system design procedure for a building structure on the basis of the measurement of the top floor absolute acceleration response. The procedure employs the H$^\infty$ proper controller and its effectiveness is favorably compared with the strictly proper controller for the impulse input excitation. Following the computer simulations using the sinusoidal excitations, the validity of the presented H$^\infty$ proper controller design is experimentally demonstrated for the four-story structural building by the sinusoidal and earthquake disturbances.

KEYWORDS

H$^\infty$ control, absolute acceleration measurement, proper controller

INTRODUCTION

With the recent rapid progress and development of modern technology, civil engineers are getting to change the strategies to ensure the structural safety, reliability and serviceability in case of earthquakes. Active structural control application to building structures is one of such typical examples. In fact, the idea of actively controlled structure has recently appealed to structural engineers all over the world, as a new promising tool for improving the seismic reliability of structures.
For the structural control application to a building structure, the output feedback is a matter of necessity for the building structural control because the structure involves too many states to be measured. And thus the so-called state feedback control is not realistic.

The present investigation deals with H$^\infty$ structural control design utilizing the absolute acceleration response measurement of the top floor of a building. The H$^\infty$ control application to a building was discussed by several researchers(Nonami *et al.*, 1992, Watanabe and Yoshida, 1992, Nishitani and Yamada, 1993). These researches were not based on the absolute acceleration measurement. The absolute acceleration measurement has a couple of advantageous characteristics: (1)accelerometers are easily available and are not very big in comparison with the direct velocity measurement devices; (2) if the usage of an accelerometer is presumed, the absolute acceleration measurement will be easier to be performed partially because it does not have to get through any integral procedure for getting velocity, and partially because, unlike the relative acceleration measurement, it is directly measured without

the measurement of ground acceleration involved. Spencer and his colleagues have been recently doing theoretical and experimental research activities utilizing the absolute acceleration measurement based on the H^2 control theory (Spencer *et al.*, 1991, 1994 and Dyke *et al.*, 1994).

In this paper, the H^∞ structural control procedure based on the absolute acceleration measurement of the top floor is presented for a building with AMD(Active Mass Damper) on the top floor. The procedure employs the H^∞ proper controller and its effectiveness is examined by the impulse input excitation. In addition, H^∞ control performance is demonstrated for the sinusoidal and earthquake disturbances by achieving the simultaneous response control of the first and second modes with robust stability.

ABSOLUTE ACCELERATION MEASUREMENT BASED CONTROL

Modeling of Structural Control System

The model of an n-story building structure depicted in **Fig.1** is considered. For the structural control system with the measurement of the absolute acceleration, the original state-space representation is formulated in the following fashion:

$$\left.\begin{aligned} \dot{x}_s &= A_S\, x_s + B_S\, u + E_S\, \ddot{q} \\ y &= C_S\, x_s + D_S\, u \end{aligned}\right\} \tag{1}$$

where $x_s = [x_1, x_2, \ldots, x_n, x_a, \dot{x}_1, \dot{x}_2, \ldots, \dot{x}_n, \dot{x}_a]^T$; u = control force; $\ddot{q}$ = seismic ground acceleration; y = measured output for feedback, and A_S, B_S, E_S, C_S, D_S = matrices specifying the control system.

For the purpose of constructing the structural model for controlling the first two modes, the original formulation is converted into(Yamada, 1995) :

$$\left.\begin{aligned} \dot{\eta}_R &= A_R\, \eta_R + B_R\, u + E_R\, \ddot{q} \\ y &= C_R\, \eta_R + D_R\, u \end{aligned}\right\} \tag{2}$$

in which η_R : modal state vector, A_R, B_R, E_R, C_R, D_R = matrices specifying the reduced-order control system. For more specific description, the experimental model of a four-story building structure is utilized. The masses m, dampings c and stiffnesses k of the experimental model are : $m_1 = m_2 = m_3 = 1.47$(kg); $m_4 = 1.63$(kg); $m_a = 0.77$(kg); $c_1 = c_2 = c_3 = c_4 = 5.47$(N·sec/m); $k_1 = k_2 = k_3 = k_4 = 5170$(N/m), respectively. The natural frequencies for each mode are calculated to be $20.1, 58.3, 90.0, 111$(rad/sec) and critical damping ratios are $0.0106, 0.0308, 0.0476, 0.0588$.

H^∞ Control Strategy

Having constructed the model accounting for the first and second modes and thus assuming the existence of additive uncertainty $\Delta G(s)$, the controller design is proceeded along with the following weighting function for the robust stability :

$$W_1(s) = \kappa_1 \frac{s^2}{s^2 + 2\zeta_1\lambda_1 s + \lambda_1^2} \quad \text{with } \lambda_1 = 90.0\ ;\ \ \zeta_1 = 0.165\ ;\ \ \kappa_1 = 0.553. \tag{3}$$

For the sensitivity reduction, on the other hand, the weighting functions corresponding to the absolute acceleration response of the top floor and the relative displacement of AMD on the top floor are considered. To perform the simultaneous control of the first and second mode responses, the following weighting function representing a lowpass filter is employed:

$$W_s(s) = \frac{1}{a_2 s^2 + a_1 s + a_0} \quad \text{with } a_0 = 1.0\ ;\ \ a_1 = 1.885 \times 10^{-3}\ ;\ \ a_2 = 1.778 \times 10^{-4}. \tag{4}$$

Similar form of the weighting function corresponding to the AMD displacement is used:

$$W_a(s) = \kappa_2 W_s(s) \tag{5}$$

Combining $W_s(s)$ and $W_a(s)$ leads to the weighting function, $W_2(s)$, for the sensitivity reduction :

$$W_2(s) = \frac{1}{\beta}\begin{bmatrix} W_s(s) & 0 & 0 \\ 0 & W_a(s) & 0 \end{bmatrix} \tag{6}$$

Fig.2 schematically illustrates $W_s(s)$, $W_a(s)$, $W_1(s)$ and $\Delta G(s)$.

Comparison of three types of criteria is made to clarify their effects to control performance, and the authors pointed out the problems resulting from each criterion (Yamada and Nishitani, 1994, 1995). Among these three, the following employed by Nonami *et al.* (1992) seems to provide the most preferable control performance:

$$\left\| \begin{matrix} W_1 K(I-GK)^{-1}G_Q \\ W_2(I-GK)^{-1}G_Q \end{matrix} \right\|_\infty < 1 \tag{7}$$

where G = transfer function from control force to measured output; G_Q = transfer function from ground acceleration to measured output; K = transfer function from output to control force; $\| \|_\infty$ = the H^∞ norm. This paper thereupon employs the above criterion in performing the H^∞ structural control system design. In association with (2)(3)(6) and (7) , the absolute acceleration measurement based H^∞ control system is formulated. Following the conventional matrix-styled notation, the coefficients governing (9) can be expressed as:

$$\left[\begin{array}{c|c:c} A & B_1 & B_2 \\ \hline C_1 & D_{11} & D_{12} \\ \hdashline C_2 & D_{21} & D_{22} \end{array}\right] = \left[\begin{array}{ccc|c:c} A_{W1} & \emptyset & \emptyset & \emptyset & B_{W1} \\ \emptyset & A_{W2} & B_{W2}C_R & \emptyset & B_{W2}D_R \\ \emptyset & \emptyset & A_R & E_R & B_R \\ \hline C_{W1} & \emptyset & \emptyset & \emptyset & D_{W1} \\ \emptyset & C_{W2} & D_{W2}C_R & \emptyset & D_{W2}D_R \\ \hdashline \emptyset & \emptyset & C_R & \emptyset & D_R \end{array}\right] \tag{8}$$

where $A_{W1}, B_{W1}, C_{W1}, D_{W1}, A_{W2}, B_{W2}, C_{W2}$ and D_{W2} are obtained by converting W_1 and W_2 into the state-space representations.

H^∞ PROPER CONTROLLER DESIGN BASED ON ABSOLUTE ACCELERATION MEASUREMENT

In employing the absolute acceleration measurement for H^∞ output feedback control, the state-space representation is formulated by:

$$\left.\begin{aligned} \dot{x} &= Ax + B_1 w + B_2 u \\ z &= C_1 x + D_{11} w + D_{12} u \\ y &= C_2 x + D_{21} w + D_{22} u \end{aligned}\right\} \tag{9}$$

The third equation, known as the output equation, carrys the control-force related term, $D_{22}u$. To get rid of this, $\bar{y}$ is newly utilized in stead of y:

$$\bar{y} = y - D_{22}u \tag{10}$$

Utilizing $\bar{y}$, the H^∞ output feedback controller can be written as:

$$\dot{\xi} = \hat{A}\xi + \hat{B}\bar{y}\,; \quad u = \hat{C}\xi \tag{11}$$

The algorithm for obtaining $\hat{A}, \hat{B}$ and $\hat{C}$ has been proposed by Sampei *et al.*(1990). Utilizing (10), the first part of (11) leads to:

$$\dot{\xi} = (\hat{A} - \hat{B}D_{22}\hat{C})\xi + \hat{B}y$$

Then the strictly proper controller associated with the absolute acceleration measurement is given by:

$$\dot{\xi} = (\hat{A} - \hat{B}D_{22}\hat{C})\xi + \hat{B}y \; ; \; u = \hat{C}\xi \tag{12}$$

This paper deals with AMD installed on the top floor. However, one has sometimes difficulty in utilizing AMD as a strictly proper controller. That is, the center of AMD's motion would move away from its initial position, and thus could not provide desired control forces. To clear away such a trouble, the relative displacement and velocity of AMD with respect to the top floor are also included in the measured outputs, i.e., the following outputs are to be measured for the feedback:

• top floor absolute acceleration; • relative displacement of AMD; • relative velocity of AMD.

This is because static feedback gains for the AMD displacement and velocity are to provide the same effects as a kind of stiffness and damping. More specifically, the control force is represented by:

$$u = v + \widehat{D}y \tag{13}$$

which gives a proper controller with $\widehat{D}$ = constant gain and v = dynamic control force $\hat{C}\xi$. It should be noted that $\hat{C}\xi$ is expressed as v for the proper controller. Then the output equation of (9) is converted into

$$y = (I - D_{22}\widehat{D})^{-1}C_2x + (I - D_{22}\widehat{D})^{-1}D_{21}w + (I - D_{22}\widehat{D})^{-1}D_{22}v \tag{14}$$

Substituting (13) and (14) into (9) and repeating the similar calculations, one has

$$\left.\begin{aligned} \dot{x} &= A^{\#}x + B_1^{\#}w + B_2^{\#}v \\ z &= C_1^{\#}x + D_{11}^{\#}w + D_{12}^{\#}v \\ y &= C_2^{\#}x + D_{21}^{\#}w + D_{22}^{\#}v \end{aligned}\right\} \tag{15}$$

where the coefficients with the superscript # are, arranged in order of derivation,

$$\begin{array}{lll} C_2^{\#} = (I - D_{22}\widehat{D})^{-1}C_2; & D_{21}^{\#} = (I - D_{22}\widehat{D})^{-1}D_{21}; & D_{22}^{\#} = (I - D_{22}\widehat{D})^{-1}D_{22}; \\ A^{\#} = A + B_2\widehat{D}C_2^{\#}; & B_1^{\#} = B_1 + B_2\widehat{D}D_{21}^{\#}; & B_2^{\#} = B_2 + B_2\widehat{D}D_{22}^{\#}; \\ C_1^{\#} = C_1 + D_{12}\widehat{D}C_2^{\#}; & D_{11}^{\#} = D_{11} + D_{12}\widehat{D}D_{21}^{\#}; & D_{12}^{\#} = D_{12} + D_{12}\widehat{D}D_{22}^{\#} \end{array} \tag{16}$$

with I = identity matrix. Once $A^{\#} \sim D_{22}^{\#}$ in (15) have been obtained, one can deal with (9) by replacing $A \sim D_{22}$ in (9) by them and thus can calculate the control force, v, by treating

$$\dot{\xi} = (\hat{A} - \hat{B}D_{22}^{\#}\hat{C})\xi + \hat{B}y \; ; \; v = \hat{C}\xi \tag{17}$$

Based on the above discussion the fundamental procedure to obtain the H^{∞} proper controller with the absolute acceleration measurement can be reduced to the following steps: (i) appropriately choose $\widehat{D}$; (ii) calculate $A^{\#} \sim D_{22}^{\#}$ by means of (8) to deal with (15) instead of (9); (iii) obtain $\hat{A}, \hat{B}, \hat{C}$ considering $D_{22}^{\#} = 0$; (iv) determine $v = \hat{C}\xi$ from (17); (v) add $\widehat{D}y$ to v and then get $u = v + \widehat{D}y$;

EXAMPLE

Proper Controller Effects for the Impulse Input Tests

For the purpose of examining the effectiveness of the proper controller, experiments and computer simulations are conducted for a model building subjected to an impulse excitation.

For the model building with the parameters shown in **Fig.1**, $\widehat{D} = [\ 0 \quad -100 \quad 0\ ]$ is employed as the static gain for the proper controller. The strictly proper controller is easily provided by setting $\widehat{D} = [\ 0 \quad 0 \quad 0\ ]$. Along with an initial displacement of AMD = 5(mm) experiments are executed. **Figs.3-5** show the time histories of the top floor acceleration response, the control force and the AMD displacement for proper controller, respectively. For the case of the strictly proper controller **Figs.6-8** represent the same time histories as **Figs.3-5**. Although recognizing only non-significant difference between both controllers in terms of the top-floor responses and the control forces, AMD for the proper controller easily or smoothly goes back to the initial position before and after the impulse excitation whereas the strictly proper controller does not.

Computer simulations are operated with the same conditions as the experiments. **Figs.9-11** show the results plotted together for the proper and strictly proper controllers, presenting the top floor acceleration responses, the control forces and the AMD displacements, respectively. Like the experiments, it is also noted that AMD has difficulty to get back to the initial position for the strictly proper controller.

Control Performance for the Sinusoidal and Earthquake Disturbances

Experimental verification for the presented proper controller design procedure with the absolute acceleration measurement is conducted. **Fig.12** shows the theoretical uncontrolled and controlled transfer functions from the seismic acceleration, $\ddot{q}$, to the top floor absolute acceleration response, $\ddot{x}_4 + \ddot{q}$, thus indicating the successful reduction of the first and second mode responses without exciting the third mode. In addition, the phase characteristics shown in **Fig.12** demonstrates that additive damping effect was obtained without changing the natural frequencies.

Fig.13 provided experimental results obtained by conducting shaking table tests. **Fig.13** depicts the transfer function from $\ddot{q}$ to $\ddot{x}_4 + \ddot{q}$ with and without control. These experimental results seem to be in good agreement with the theoretical results shown in **Fig.12**. **Fig.14** shows the controlled and uncontrolled absolute acceleration time histories of the top floor of the experimental model subjected to the Northern Miyagi Prefecture earthquake, with considerable control effect presented. **Fig.15** denotes the simulated absolute acceleration of the top floor based on the the earthquake input observed by the accelerometer attached to the bottom of the structure. It is noted that almost the same control performance is achieved as the experimental result.

CONCLUDING REMARKS

This paper discussed the H^∞ proper controller design procedure with the absolute acceleration measurement. The results shown in this paper are summarized as follows. (1) Design procedures was technically and explicitly presented for the absolute acceleration measurement strategy with proper controller. (2) It is indicated that one has sometimes difficulty in utilizing AMD as a strictly proper controller from the impulse response experiments and computer simulations, and H^∞ proper controller has been developed to improve AMD's motion. (3) By applying the design procedure with the H^∞ proper controller to the four-story building subjected to sinusoidal and earthquake disturbances, not only efficient damping effect was obtained without changing the natural frequencies, it was also shown that multi-mode robust control was successfully provided with the control devices installed only at the top floor.

ACKNOWLEDGEMENT

This research is partially supported by Ministry of Education 1994 Grant-in-Aid Encourage Research for Young Scientist # 065217.

REFERENCES

Dyke, S.J., B.F. Spencer Jr., P. Quast, M.K. Sain and S.C. Kaspari Jr. (1994). Experimental verification of acceleration feedback control strategies for MDOF structures. *Proceedings, the Second International Conference on Computational Stochastic Mechanics*, Athens, Greece.

Nishitani, A. and N. YAMADA (1993). Rebirth of rontrol with frequency domain viewpoint. *Proceedings, International Workshop on Structural Control*, Hawaii, 360-366.

Nonami, K., H. Nishimura and W. Cui (1992). H^∞ control of multi-degree-of-freedom systems using active dynamic vibration absorber (A criterion for design of frequency weighting function) (in Japanese). *Transaction on JSME, C*, Vol.58, No.548, 1311-1317.

Sampei, M., T. Mita and M. Nakamichi (1990). An algebraic approach to H^∞ output feedback control problems. *System & Control Letters, 14*, North-Holland, 13-24.

Spencer Jr., B.F., J. Suhardjo and M.K. Sain (1991). Frequency domain control algorithms for civil engineering applications. *Proceedings, International Workshop on Technology for Hong Kong's Infrastructure Development*, Hong Kong, 169-178.

Spencer Jr., B.F., J. Suhardjo and M.K. Sain (1994). Frequency domain optimal control strategies for aseismic protection. *Journal of Engineering Mechanics, ASCE*, Vol.120, No.1, 135-159.

Watanabe, T. and K. Yoshida (1992). The consideration and comparisons of various robust control rules for a multi-degree-of-freedom structure using active dynamic vibration absorber (in Japanese). *Transaction on JSME, C*, Vol.58, No.546, 78-84.

Yamada, N. and A. Nishitani (1994). H^∞ structural control design considering selection of design criteria and controller reduction (in Japanese). *Journal of Structural and Construction Engineering, AIJ, 462*, 21-29.

Yamada, N. (1995). H^∞ structural control system design for building structures (in Japanese). D.Eng. dissertation, Waseda University, Tokyo, Japan,

Yamada, N. and A. Nishitani (1995). H^∞ structural control system design based on absolute acceleration measurement. *Proceedings, 1995 Design Engineering Technical Conferences, Volume-3, C, ASME*, 433-438.

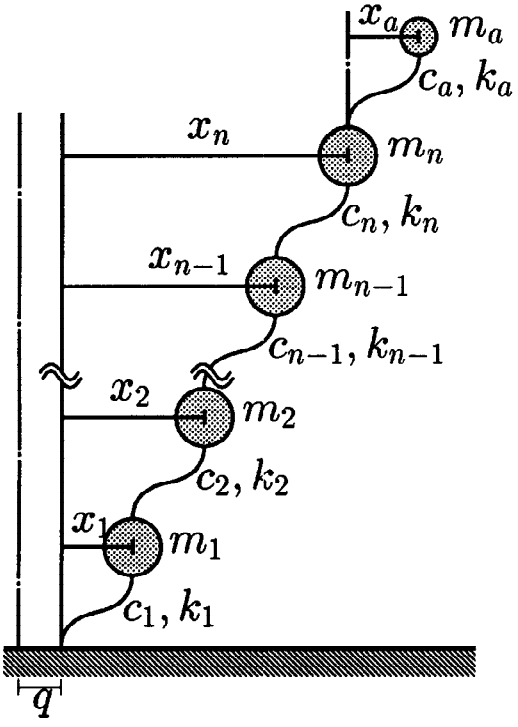

FIG. 1 Configuration of structural model

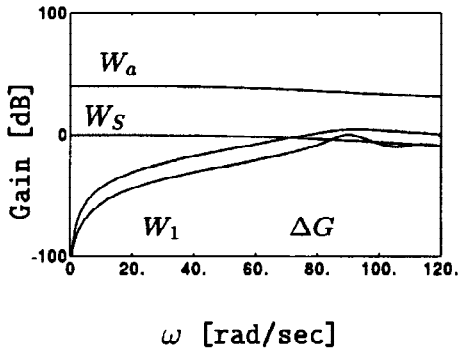

FIG. 2 Magnitudes of $W_s(s), W_a(s)$ and σ-plots of $\Delta G(s), W_1(s)$

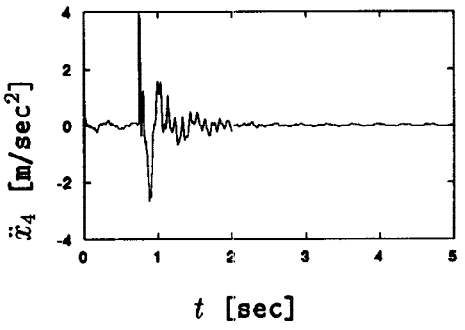

FIG. 3 Top floor acceleration with proper controller

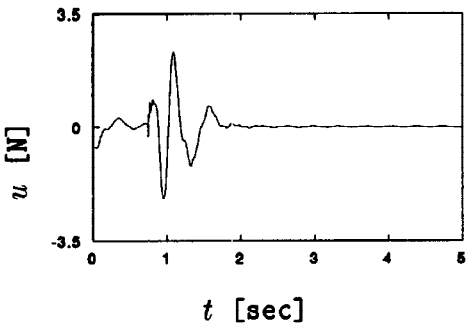

FIG. 4 Control force with proper controller

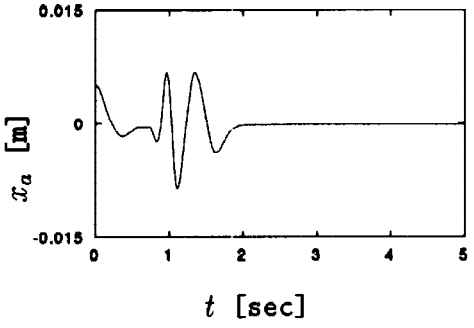

FIG. 5 AMD displacement with proper controller

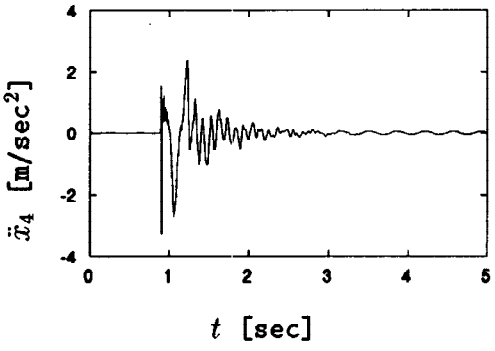

FIG. 6 Top floor acceleration with strictly proper controller

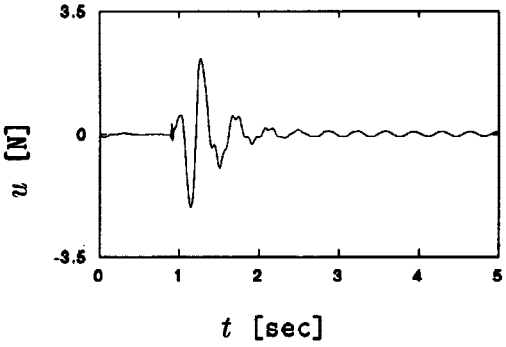

FIG. 7 Control force with strictly proper controller

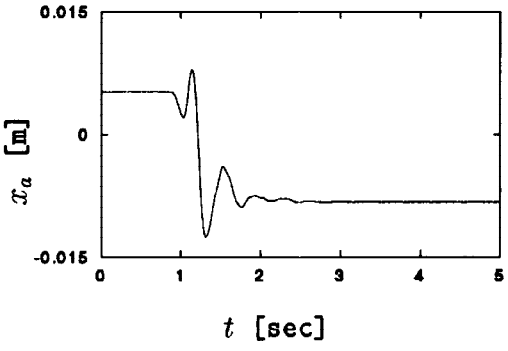

FIG. 8 AMD displacement with strictly proper controller

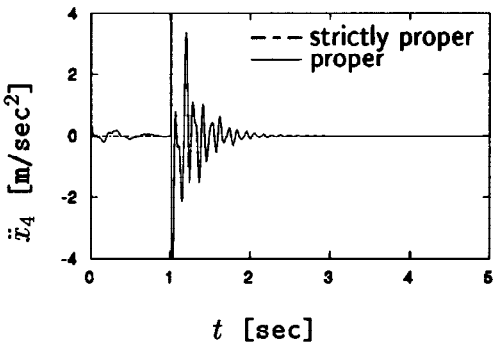

FIG. 9 Comparison of top floor accelerations

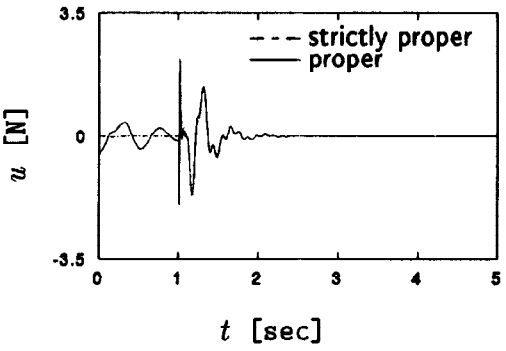

FIG. 10 Comparison of control forces

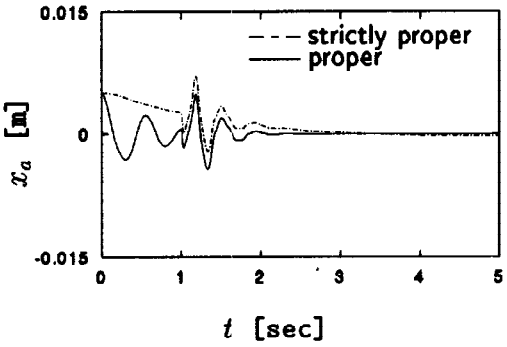

FIG. 11 Comparison of AMD displacements

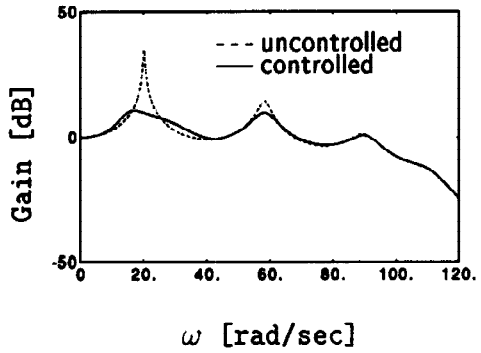

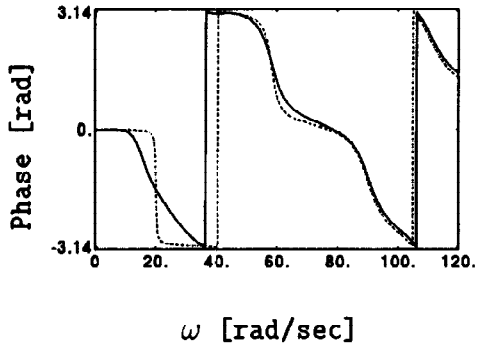

FIG. 12 Frequency response of absolute acceleration at the top floor

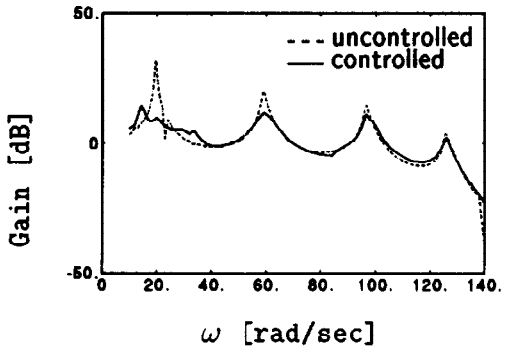

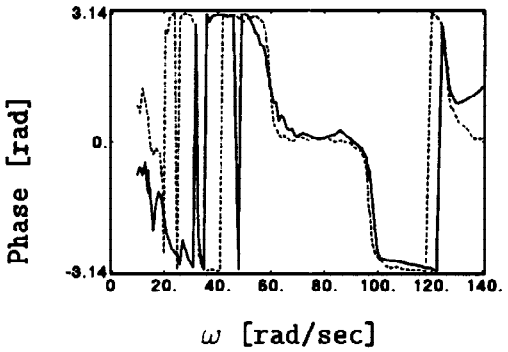

FIG. 13 Frequency response from ground acceleration to the top floor absolute acceleration

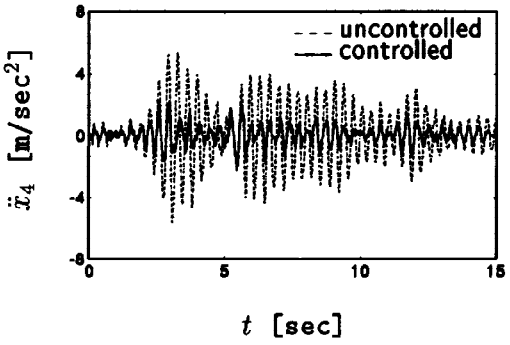

FIG. 14 The top floor absolute acceleration for Northern Miyagi prefecture earthquake

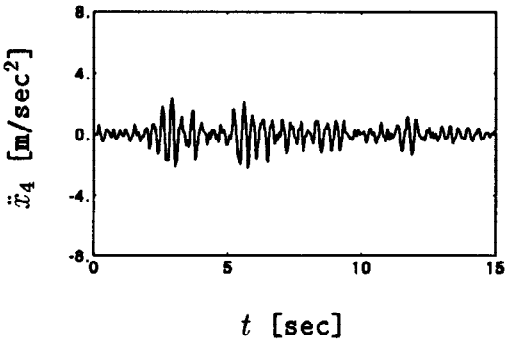

FIG. 15 The top floor absolute acceleration for Northern Miyagi prefecture earthquake